THE EFFECT OF SURFACE REGRESSION ON THE DOWNWARD FLAME SPREAD OVER A SOLID FUEL IN A QUIESCENT AMBIENT

by

Mohammad B. AYANI, Javad A. ESFAHANI, and Antonio C. M. SOUSA

Original scientific paper
UDC: 662.992.8
BIBLID: 0354-9836, *11* (2007), 2, pp. 67-86

The present work is addressed to the numerical study of the transient laminar opposed-flow flame spread over a solid fuel in a quiescent ambient. The transient governing equations – full Navier-Stokes, energy, and species (oxygen and volatiles) for the gas phase, and continuity and energy equations for the solid phase (fuel) with primitive variables are discretized in a staggered grid by a control volume approach. The second-order Arrhenius kinetics law is used to determine the rate of consumption of volatiles due to combustion, and the zero-order Arrhenius kinetics law is used to determine the rate of degradation of solid fuel. The equations for the fluid and solid phases are solved simultaneously using a segregated technique. The physical and thermo-physical properties of the fluid (air) such as density, thermal conductivity, and viscosity vary with temperature. The surface regression of the solid fuel is modeled numerically using a discrete formulation, and the effect upon the results is analyzed. The surface regression of the solid fuel as shown affects on the fuel surface and gas temperature, mass flux and velocity of volatiles on the top surface of fuel, total energy transferred to the solid phase, etc. It seems the results to be realistic.

Key words: *flame spread, downward, polymethyl methacrylate,, surface regression, computational fluid dynamics, ignition*

Introduction

Flame spread over solid fuel surfaces has been a subject of intensive experimental and theoretical investigations [1-15] due to its importance to fire safety. A review of modeling and simulation of combustion processes of charring and non-charring solid fuels was be done by Di Blasi [1]. Wichman [2] reviewed the theory of opposed-flow flame spread. Fernandez-Pello and Williams [3] studied experimentally laminar flame spread over polymethyl methacrylate (PMMA) surfaces. They measured spread rates, temperature and velocity field for various thicknesses of fuel. Mao *et al*. [4] numerically studied the downward flame spread over thin solid of PMMA. They solved the steady-state, two dimensional, laminar non radiative conservation equations of mass, momentum, energy, and species for volatiles and oxygen in the gas phase.

The numerical study of flame spread over solid materials in a quiescent environment in microgravity was investigated by Bhattachrjee *et al.* [5]. They attached the coordinate system to the solid surface and used the steady-state of governing equations for both solid and gas phases. Also Bahattacharjee and Altenkirch [6] studied the effect of radiation on opposed-flow flame spread over thin solid fuel in a microgravity environment. They showed that at low opposing flow velocities, the radiation effects become significant and are manifested in lowered spread rates and cooler and smaller flames. At higher opposing flow, these effects disappear, justifying the neglect of radiation in most forced and natural convection situation in normal gravity produced by thin fuel.

Di Blasi *et al*. [7] studied the ignition processes of polymeric materials with gas-phase absorption of radiation. They used the unsteady-one-dimensional form of the governing equations for both solid and gas phases. Bahattacharjee and Altenkirch [8] compared the theoretical and experimental results in flame spread over thin condensed fuels in a quiescent, microgravity environment. They showed that the theory compares well with experimental near the flame leading edge. Ramachandra *et al.* [9] studied the behavior of flame spreading over thin solid in microgravity by experimental methods. They studied the effect of oxygen concentration and pressure of quiescent environment on the phenomenon. Their experimental results show that the spread rate increases with ambient oxygen level and pressure. Bhattacharjee *et al.* [10] used experimental and computational methods to study the effect of ambient pressure on the flame spread over thin cellulose fuels in a quiescent microgravity environment. Jiang *et al*. [11] numerically studied the steady upward flame spread over a thin solid in reduced gravity. They showed that in the reduced gravity, the gaseous flame radiation is important for flame structure, flame dimension, and extinction limit.

The unsteady flame spread to extinction over thick fuels in microgravity was studied numerically by Altenkirch *et al*. [12]. They solved the governing equations for both solid and gas phases separately.

Esfahani and Sousa [13] studied numerically the ignition of epoxy by a high radiation source. They solved the transient two dimensional governing equations for both gas and solid phases separately. They can estimate the ignition delays for epoxy. Sousa and Esfahani [14] also studied by numerical methods the ignition of PMMA which induced by monochromatic radiation. In recent work, Esfahani [15-17] studied the effect of oxygen concentration on the degradation of PMMA by numerical methods.

In the most of the previous works, the governing equations solved for gas and solid phases separately and coupling the solution for the solid and gas phases through the boundary conditions at the gas-solid interface. Also in all of the previous works, some of the researches studied just the ignition delay and some of them studied just the rate of flame spread over solid fuel. In this study, it is tried to solve the transient two-dimensional governing equations for both gas and solid phases simultaneously. The pilot ignition has been used to achieve the burning situation. The present model has capability to study both the ignition delay and the flame spread over solid fuel. Also in this study, the effect of surface regression of the solid is considered, while in previous work, its effect is assumed to be negligible. The proposed model is suitable to predict the flow field and flame spread over all thicknesses of solid fuel.

Mathematical model

Figure 1 shows the computational domain, and the relative location of the solid fuel. The fuel is represented by a vertical thin and long (thickness equals 0.001 m and height equals 0.02 m) of non charring solid fuel (PMMA) on the left bottom corner of the computational domain. The computational domain is performed over a 0.1 m height (x direction) by 0.03 m wide (y direction). The mathematical model is based on the partial differential equations for conservation of mass, momentum, energy, and species in the gas and solid phases. The coordinate system is fixed relative to the computational domain, therefore it should be used the unsteady form of the governing equations. The two dimensional transient governing equations in the gas phase are as follows:

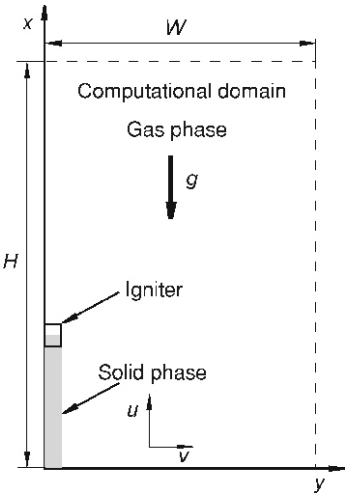

Figure 1. Schematic of computational domain and coordinate system

– *Continuity equation*

$$\frac{\partial \rho}{\partial t} \quad (\rho \vec{\mathrm{V}}) \quad 0 \tag{1}$$

where

$$\vec{\mathrm{V}} \quad u\vec{\mathrm{i}} \quad v\vec{\mathrm{j}} \tag{2}$$

– *Momentum in x direction*

$$\frac{\partial (\rho u)}{\partial t} \quad \frac{\partial (\rho u^2)}{\partial x} \quad \frac{\partial (\rho uv)}{\partial y} \quad X \quad \frac{\partial p}{\partial x} \quad \frac{\partial \sigma_{\mathrm{x}}}{\partial x} \quad \frac{\partial \tau_{\mathrm{yx}}}{\partial y} \tag{3}$$

– *Momentum in y direction*

$$\frac{\partial (\rho v)}{\partial t} \quad \frac{\partial (\rho uv)}{\partial x} \quad \frac{\partial (\rho v^2)}{\partial y} \quad \frac{\partial p}{\partial y} \quad \frac{\partial \tau_{xy}}{\partial x} \quad \frac{\partial \sigma_y}{\partial y} \tag{4}$$

where

$$\sigma_{\mathrm{x}} \quad \frac{2}{3}\mu \quad \vec{\mathrm{V}} \quad 2\mu \frac{\partial u}{\partial x} \tag{5}$$

$$\sigma_{\mathrm{y}} \quad \frac{2}{3}\mu \quad \vec{\mathrm{V}} \quad 2\mu \frac{\partial v}{\partial y} \tag{6}$$

$$\tau_{\mathrm{xy}} \quad \tau_{\mathrm{yx}} \quad \mu \quad \frac{\partial v}{\partial x} \quad \frac{\partial u}{\partial y} \tag{7}$$

In eq. (3), X is the body force per unit volume in the x direction. The energy equation with the assumption of constant specific heat at constant pressure for gas phase is:

– *Energy equation*

$$\frac{\partial(\rho T)}{\partial t} \quad \frac{\partial(\rho u T)}{\partial x} \quad \frac{\partial(\rho v T)}{\partial y} \quad \frac{1}{c_{\mathrm{p}}} \quad (k \quad T) \quad \frac{\dot{G}}{c_{\mathrm{p}}} \tag{8}$$

where $\dot{G}$ is the rate of energy generation due to chemical reaction which can be determined from the following relation:

$$\dot{G} = - S_{\mathrm{F}} \Delta h \tag{9}$$

In the energy equation, it is assumed the viscous dissipation and the net heat loss by radiation to be negligible [6].

– *Species equations*

for fuel:

$$\frac{\partial(\rho Y_{\mathrm{F}})}{\partial t} \quad \frac{\partial(\rho u Y_{\mathrm{F}})}{\partial x} \quad \frac{\partial(\rho v Y_{\mathrm{F}})}{\partial y} \quad \frac{\partial}{\partial x} \quad \rho D_{\mathrm{AB}} \frac{\partial Y_{\mathrm{F}}}{\partial x} \quad \frac{\partial}{\partial y} \quad \rho D_{\mathrm{AB}} \frac{\partial Y_{\mathrm{F}}}{\partial y} \quad S_{\mathrm{F}} \tag{10}$$

and for oxygen:

$$\frac{\partial(\rho Y_{\mathrm{O}})}{\partial t} \quad \frac{\partial(\rho u Y_{\mathrm{O}})}{\partial x} \quad \frac{\partial(\rho v Y_{\mathrm{O}})}{\partial y} \quad \frac{\partial}{\partial x} \quad \rho D_{\mathrm{AB}} \frac{\partial Y_{\mathrm{O}}}{\partial x} \quad \frac{\partial}{\partial y} \quad \rho D_{\mathrm{AB}} \frac{\partial Y_{\mathrm{O}}}{\partial y} \quad S_{\mathrm{O}} \tag{11}$$

The rate of consumption of volatiles (S_{F}) due to combustion can be determined from the second-order Arrhenius kinetics law [18]:

$$S_{\mathrm{F}} \quad A_{\mathrm{g}} \mathrm{e}^{\frac{E_g}{\mathrm{R}T}} Y_{\mathrm{O}} Y_{\mathrm{F}} \rho^2 \tag{12}$$

The amount of oxygen consumed is determined by using the following relation:

$$S_{\mathrm{O}} \quad S_{\mathrm{F}} \nu_{\mathrm{O}} \frac{M_{\mathrm{O}}}{M_{\mathrm{F}}} \tag{13}$$

The transient two dimensional equations governing the conservation of mass and energy for the solid phase are:

– *Continuity equation*

$$\frac{\partial m}{\partial x} \quad S_{\mathrm{v}}\rho_{\mathrm{s}} \tag{14}$$

– *Energy equation*

$$\rho_{\mathrm{s}}c_{\mathrm{s}}\frac{\partial T_{\mathrm{s}}}{\partial t} \quad (T_{\mathrm{s}} \quad T_{\mathrm{i}})\rho_{\mathrm{s}}S_{\mathrm{v}}(c_{\mathrm{v}} \quad c_{\mathrm{s}}) \quad m\ c_{\mathrm{v}}\frac{\partial T_{\mathrm{s}}}{\partial x}$$
$$= \frac{\partial}{\partial x}\ k_{\mathrm{s}}\frac{\partial T_{\mathrm{s}}}{\partial x} \quad \frac{\partial}{\partial y}\ k_{\mathrm{s}}\frac{\partial T_{\mathrm{s}}}{\partial y} \quad \rho_{\mathrm{s}}S_{\mathrm{v}}\Delta H_{\mathrm{v}} \tag{15}$$

In this equation it is assumed the volatiles within the solid moves only in the x direction. The rate of volatiles generation in the solid can be determined from the zero-order Arrhenius kinetics law [18]:

$$S_{\mathrm{v}} \quad A_{\mathrm{s}}\mathrm{e}^{\ \frac{E_{\mathrm{s}}}{\mathrm{R}T_{\mathrm{s}}}} \tag{16}$$

The total volatiles flux from the surface of the solid can be determined from eq. (14):

$$m \quad \int_0^L S_{\mathrm{v}}\rho_{\mathrm{s}}\mathrm{d}x \tag{17}$$

Also the variation of solid density *vs.* time due to degradation can be determined from the following relation:

$$\frac{\partial\rho_{\mathrm{s}}}{\partial t} \quad S_{\mathrm{v}}\rho_{\mathrm{s}} \tag{18}$$

The flow is assumed to be incompressible in what concerns the variation of density with pressure; however the variation of density of the gas phase with temperature is taken into account, and is determined from the following relation:

$$\rho T = \rho_{\infty}T_{\infty} \tag{19}$$

The variation of viscosity of air with temperature is determined from Sutherland's law [19], as follows:

$$\mu \quad 1.458\ \ 10^{\ 6}\frac{\sqrt{T^3}}{T \quad 110.4} \quad [\mathrm{Ns/m^2}] \tag{20}$$

The variation of the specific heat at constant pressure, c_{p} and of the Prandtl number (Pr), of air with the temperature is practically negligible, therefore, c_{p} and Pr are assumed to be constant within the temperature; with this assumption, the variation with

temperature of the thermal conductivity for the gas phase is determined through the value of μ by using the relation:

$$k \quad \frac{c_p \mu}{\mathrm{Pr}} \tag{21}$$

Initial and boundary conditions

The initial conditions for the velocity components, temperature, and species are follows:

$$u(x, y, 0) = 0, \quad v(x, y, 0) = 0, \quad T(x, y, 0) = T_\infty, \quad Y_F(x, y, 0) = 0,$$

$$Y_O(x, y, 0) = Y_{O\infty} \quad \text{in the gas phase,} \quad \text{and} \quad Y_O(x, y, 0) = 0 \quad \text{in the solid phase} \tag{22}$$

where concentration of oxygen in the solid phase keep zero during the process.

The igniter is placed on a small zone in the gas-solid interface on the top of the solid, and its power input per unit volume is $3.5 \cdot 10^8$ W/m^3. The total power input of igniter per unit length of fuel depth is about 190 W/m. This power input is started at time zero, and is continued until flame ignition occurs, which is usually around 2 s, and beyond this time, it is shut off. For this process the flow is assumed to be symmetric about a vertical plane passing through the center of the solid fuel (fig. 1), therefore only one half plane will be considered. The boundary conditions for the symmetry plane ($y = 0$) are as follows:

$$v \quad 0 \qquad \text{and} \qquad \frac{\partial u}{\partial y} \quad \frac{\partial T}{\partial y} \quad \frac{\partial Y_F}{\partial y} \quad \frac{\partial Y_O}{\partial y} \quad 0 \tag{23}$$

The other boundaries are located relatively far away from the heat source, and the pressure is assumed to have a constant value. In this study the relative pressure is taken as zero ($p_\infty = 0$). Two types of conditions for the energy and species equations are used at the "far-field" boundaries, namely:

$$T \quad T_\infty, \quad Y_O \quad Y_{O\infty}, \quad Y_F \quad 0 \qquad (\text{inflow}) \tag{24}$$

$$\frac{\partial T}{\partial n} \quad \frac{\partial Y_O}{\partial n} \quad \frac{\partial Y_F}{\partial n} \quad 0 \qquad (\text{outflow}) \tag{25}$$

where n is the direction perpendicular to the surface of the boundaries.

Numerical method

The non-linear coupled partial differential equations are integrated by the control volume formulation to obtain the discretized equation set [20, 21]. The convec-

tive/diffusive link coefficients are based on the second order upwind scheme [22]. The governing equations were discretized for uniform staggered grids in the solid phase and non-uniform staggered grids in the gas phase, which reach their smallest value at the gas-solid interface. The expansion coefficients for the dimension of meshes in the gas phase are chosen so that the maximum aspect ratio of meshes is less than 5 in the whole of computational domain. The discretized equations for fluid and solid (fuel) phases were solved simultaneously. The values of the components velocity and the concentration of volatiles and oxygen in the solid phase are set zero by choose of suitable source terms in the discretized momentum and species conservation equations [20]. A line-by-line TDMA iterative method [20] was used to solve the discretized governing (algebraic) equations.

To avoid eventual divergence in the iterative solution, in the early times the under-relaxation factors of 0.45, 0.45, 0.55, 0.7, 0.7, and 0.55 were used for u, v, p, T, Y_F, and Y_O, respectively, and beyond ignition, time equals 2 s, their values reduce to 0.3, 0.3, 0.5, 0.4, 0.4, and 0.4. These values of under-relaxation give adequate rate of convergence for the solution of governing equations.

It is assumed that the regression of the solid takes place just on the top surface of the solid fuel. The reduction of solid density with respect to time due to degradation can be calculated from eq. (18) and then also the density of the first row meshes on the top solid fuel reduces continuously as time elapses. When the density of these meshes was being less than a criteria value, for example less than 10% of the initial density of solid, this row of meshes filled with the gas phase and next row of meshes in the solid phase takes place in the vicinity of the gas phase, and undertakes variation of its density. On the other hand the solid height reduces discretely by a solid mesh size due to burning. This trend is continued till to burn the whole of solid fuel. The flame spread rate is calculated from the following relation:

$$V_F \quad \frac{\Delta x_s}{n\Delta t} \tag{26}$$

where n is the number of interval times that taken for the first row of meshes of the solid to be burnt.

Results and discussion

To show the verification of the results, those are presented for different mesh sizes and different time steps. The variation of non-dimensional temperature of the top solid surface with respect to time for different solid mesh sizes is shown in fig. 2. In the early times before about 2 seconds, when

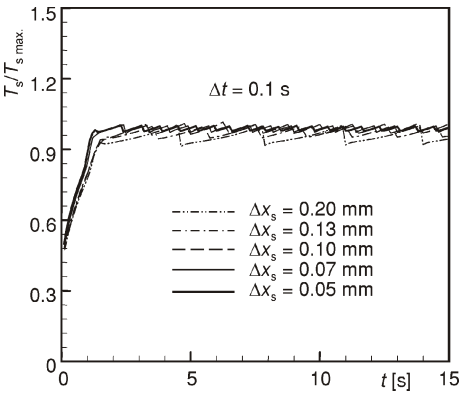

Figure 2. The variation of the non-dimensional fuel surface temperature *vs.* time for different mesh sizes for the solid region

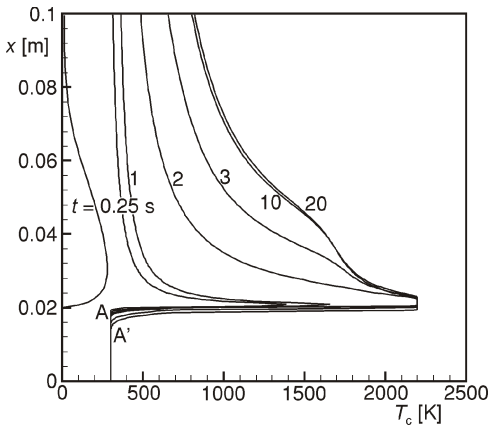

Figure 3. The variation of temperature at the symmetric plane *vs*. time

the pilot is on, the top surface temperature of the solid increases sharply. After that time, the pilot is shut off and these curves are approximately plateau. The wiggles that are seen in the plateau region of those curves are concerned to high temperature gradient of solid phase in the vicinity of gas-solid interface [3, 13, 23] and to the nation of surface regression numerical model.

Figure 3 shows the variation of the symmetric plane temperature (center line temperature) *vs.* time. The highest gradient centerline temperature takes place in the region between the gas-solid interface and combustion zone (points A and A') for all times. The location of that high gradient at the start of the processes, point A, moves downward to point A' as time passes due to moving of that interface to down, because the solid fuel burns from the top surface.

The numerical surface regression model represents the solid surface regression is take placed step by step, while the solid surface regression actually is a continues phenomenon. The proposed numerical model with using fine meshes in the solid phase could capture the high gradient solid temperature at the top solid surface and the regression phenomenon better than the model with using course meshes in solid phase. This conclusion is obviously shown in the curves of fig. 2. The amplitude of the wiggles in the plateau region is decreased with decreasing solid mesh size so that its relative value decreases from 13.4% for the solid mesh size equals 0.2 mm to less than 4% for mesh size equals 0.05 mm; this shows monotonic behavior of the numerical results and the finest grid tends to the independent limit. Of course the CPU time for the fine solid mesh is more than the course solid mesh. For example, in every day (24 hours) with the Pentium 4, 2800 MHz, the phenomenon progresses 14 seconds with the solid mesh size equals 0.2 mm, while that progress less than 1.5 seconds for the solid mesh size equals 0.05 mm *i. e*. more than 10 days need to achieve the results for fine mesh. Certainly, the results based on the course solid mesh are dependent on the solid mesh size that is caused to fair the validation of the numerical results.

Figure 4 represents the variation of solid surface temperature with respect to time for different time steps. This figure shows that the history of the solid surface temperature approximately is independent of time steps. The amplitude of wiggles is increased a little with decreasing of time step, which could be in the order of round of error.

The variation of mass flux of volatiles per unit length of solid fuel from the top solid surface with respect to time for different solid mesh sizes is shown in fig. 5. In the early times, before 1 s, the solid temperature is not enough high to begin the degradation of

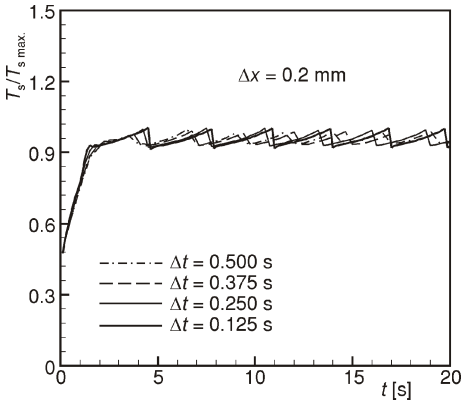

Figure 4. The variation of the non-dimensional fuel surface temperature *vs.* time for different time steps

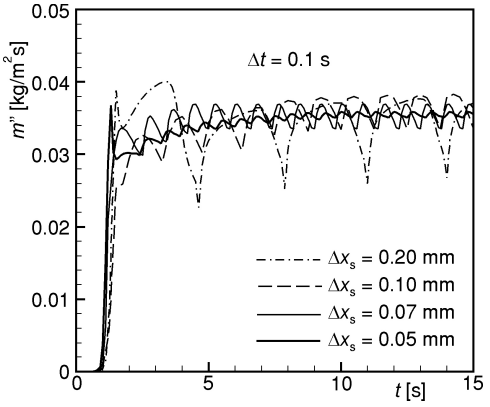

Figure 5. The variation of the mass flux of volatiles on the top surface of fuel *vs.* time

fuel and hence there is not any mass flux of volatiles on the top surface of solid fuel. But beyond that time, the degradation in the solid fuel is occurred and mass flux of volatiles increase sharply. Energy with the flow of volatiles transfers from the solid to the gas. This phenomenon causes to reduce the solid temperature and mass flux of volatiles. The wiggles in the plateau region of curves in fig. 5 are also concerned to the regression numerical model. The amplitude of wiggles is high for the solid mesh size equals 0.2 mm and its value decreases extensively by decreasing the solid mesh size so that its relative value decreases from 26.6% for the solid mesh size 0.2 mm to 2.49% for mesh size 0.05 mm. Figure 6 shows the variation of the volatiles velocity on the gas-solid interface *vs*. time. Since the mass flux of volatiles in the solid surface is proportional to volatiles velocity at that location, then the variation of them are completely similar (figs. 5 and 6).

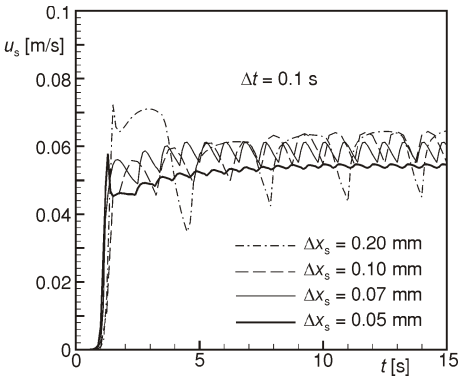

Figure 6. The variation of the velocity of volatiles on the top surface of fuel *vs.* time

Figure 7 shows the variation of solid surface temperature and gas temperature in the vicinity of that surface, and difference of those temperatures with respect to time. In the threshold of turning on pilot, the major part of the energy generation in the pilot is stored in the pilot zone and hence increases the temperature of that zone with respect to time. Since the heat capacity (ρc_p) of the gas phase is less than that of solid phase, then the gas temperature in the vicinity of solid surface is more than the solid surface temperature.

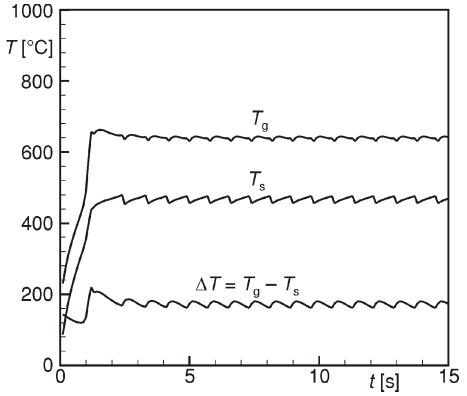

Figure 7. The variation of solid surface temperature, gas temperature in the vicinity of that surface, and temperature difference between those locations *vs.* time

Also the thermal conductivity of the gas phase (k 0.02 W/mK) is less one order of magnitude than that of the solid phase (k = = 0.2 W/mK) and the fluid around the solid phase is quiescent during that time. Thus energy of pilot in the gas phase transfers to the solid phase more than the gas phase. This action cause the rate of increasing of solid surface temperature is more than the gas temperature in the vicinity of that surface and hence the temperature difference between them decrease with respect to time till 1 second. The mass flux of volatiles after 1 second (fig. 5) and the exothermic chemical reaction begins on the vicinity of solid surface. This phenomenon causes to increase the gas temperature on that location and the temperature difference between the gas and solid phases increases till 1.2 second. After this time, the flow is begun stronger around the solid phase while the pilot is begun off. These events cause the rate of increasing of gas temperature in the vicinity of solid surface decreases and even cause to reduce the gas temperature at that location. Then the temperature difference between those two phases reduces till to reach to the plateau region.

The variation of net heat transfer to the solid phase *vs*. time (fig. 8) can be represented by the results of fig. 7. To continue of burning the solid fuel, heat must be transferred from the gas phase to the solid phase. Therefore heat transfer by diffusion from the gas phase to the solid phase must be dominated to the heat transfer by advection of the flow of volatiles on the solid surface. Since the heat diffusion between solid and gas phases is proportional to the temperature difference between them, then the variation of net heat transfer to the solid phase *vs*. time during the first second of the process is similar to the temperature difference between gas and solid phases (figs. 7 and 8). The suddenly reduction in the net heat transfer to the solid phase around 1.2 s is associated to the increasing of contribution of heat transfer by advection due to suddenly increasing mass flux of volatiles on the solid surface at that time (fig. 5). The amplitude of the wiggles in the plateau region of curves in fig. 8 is reduced with decreasing the solid mesh size. Since the heat diffusion is the dominate fac-

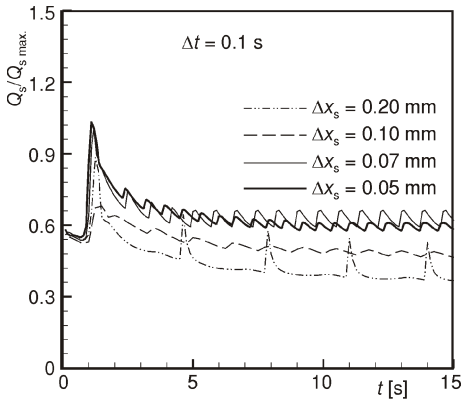

Figure 8. The variation of the heat transfer to the solid fuel *vs.* time

tor in the process and the variation of temperature in the vicinity of the interface is very sharp (fig. 3), thus it is reasonable that the net heat transfer to the solid phase extremely depends upon the solid mesh size, which is shown in the curves of fig. 8. The net heat transfer to the solid phase can be predicted more accurate by choosing smaller size for meshes.

The variation of total heat release due to combustion in the computational domain *vs*. time for different solid mesh sizes is shown in fig. 9. There is not any heat release due to combustion before 1 s but beyond this time, its value increase sharply till to reach to the plateau region. Also this figure shows that the amplitude of wiggles in the plateau region is reduced by decreasing the solid mesh size, which is consistent with previous findings.

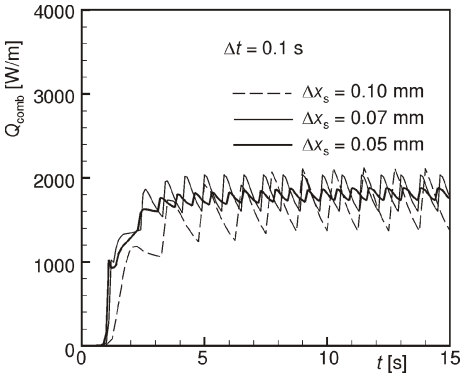

Figure 9. The variation of the total heat release due to combustion in the computational domain *vs*. time

The variation of volatiles concentration in the gas phase (Y_F) in the vicinity of the top surface of solid with respect to time for different solid mesh sizes is shown in fig.10. This figure shows the value of Y_F in that region is equal zero in the early time and beyond 1 s, its value increases sharply till to reaches the plateau region. The wiggles in that region are concerned to the numerical regression model. When a row of meshes in the top of solid phase is removed due to burning and meshes of that row filled with the gas phase, the value of Y_F decrease suddenly. The reduction of solid surface temperature (fig. 2) and reduction of mass flux of volatiles (fig. 5) at times of removing the first row meshes of the solid phase cause to reduce the value of Y_F at those times.

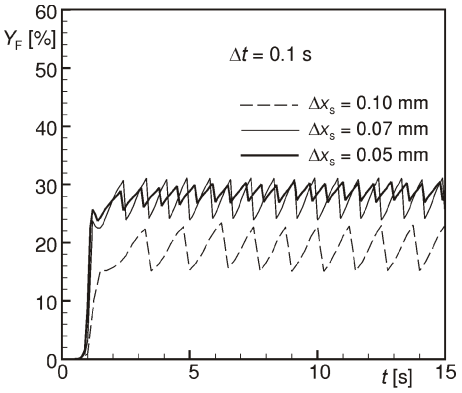

Figure 10. The variation of volatiles concentration in the vicinity of the top surface of fuel *vs*. time

The variation of oxygen concentration in the gas phase (Y_O) in the vicinity of the top surface of solid with respect to time for different solid mesh sizes is shown in fig. 11. In early times, the value of Y_O is constant and equals to the value of Y_O at the initial time. Oxygen consumes due to combustion and its concentration reduces till to reach to the plateau region. When the first row of meshes in the top of solid phase fills with the gas phase, the value of Y_F decreases and the value of Y_O increases in the vicinity of top interface as

shown in figs. 10 and 11, respectively. From those figures, it is clear that the value of Y_O is less sensitive to the solid mesh size than the value of Y_F, but both values of them tends to independent limit for the solid mesh size less than 0.07 mm.

The variation of regression rate of the solid surface (flame spread) *vs*. time for different solid mesh sizes are shown in fig. 12. This figure shows the threshold of regression increases with increasing the solid mesh size. This is physically true because the interval time for the burning of the first row meshes is proportional to the solid mesh size. This figure also represent the flame spread over solid fuel is independent of solid mesh size for mesh size smaller than 0.07 mm.

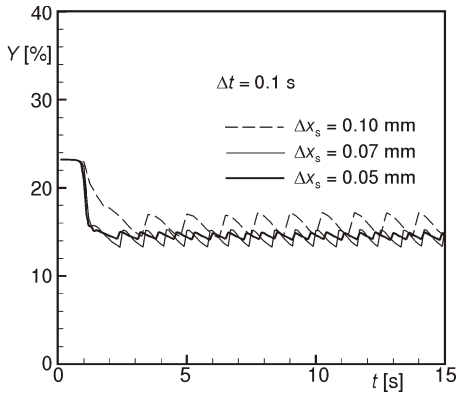

Figure 11. The variation of oxygen concentration in the vicinity of the top surface of fuel *vs*. time

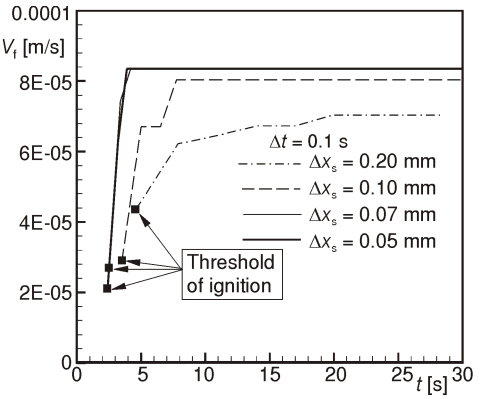

Figure 12. The variation of regression rate of the surface solid (flame spread) *vs*. time

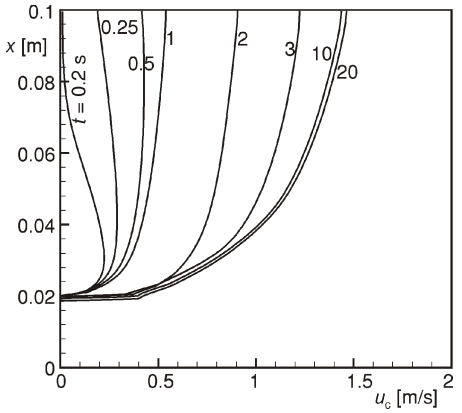

Figure 13. The variation of vertical component velocity at the symmetric plane *vs.* time

Figure 13 shows the variation of vertical component of velocity in the symmetric plane with respect to time. The moving of the top solid surface to down due to burning causes the velocity curves in the symmetric plane at 20 s moved lower than that curve at 10 s.

The growth of flow field around the solid fuel *vs*. time is shown in fig. 14 by the variation of velocity vectors in the computational domain. The biggest velocity vector is near the top surface of solid at time equals 0.1 s that it is concerned to existence of eddies in that position. As time passes, eddies grow and due to the effect of buoyancy force, they move to the top boundary of computational domain. The biggest velocity

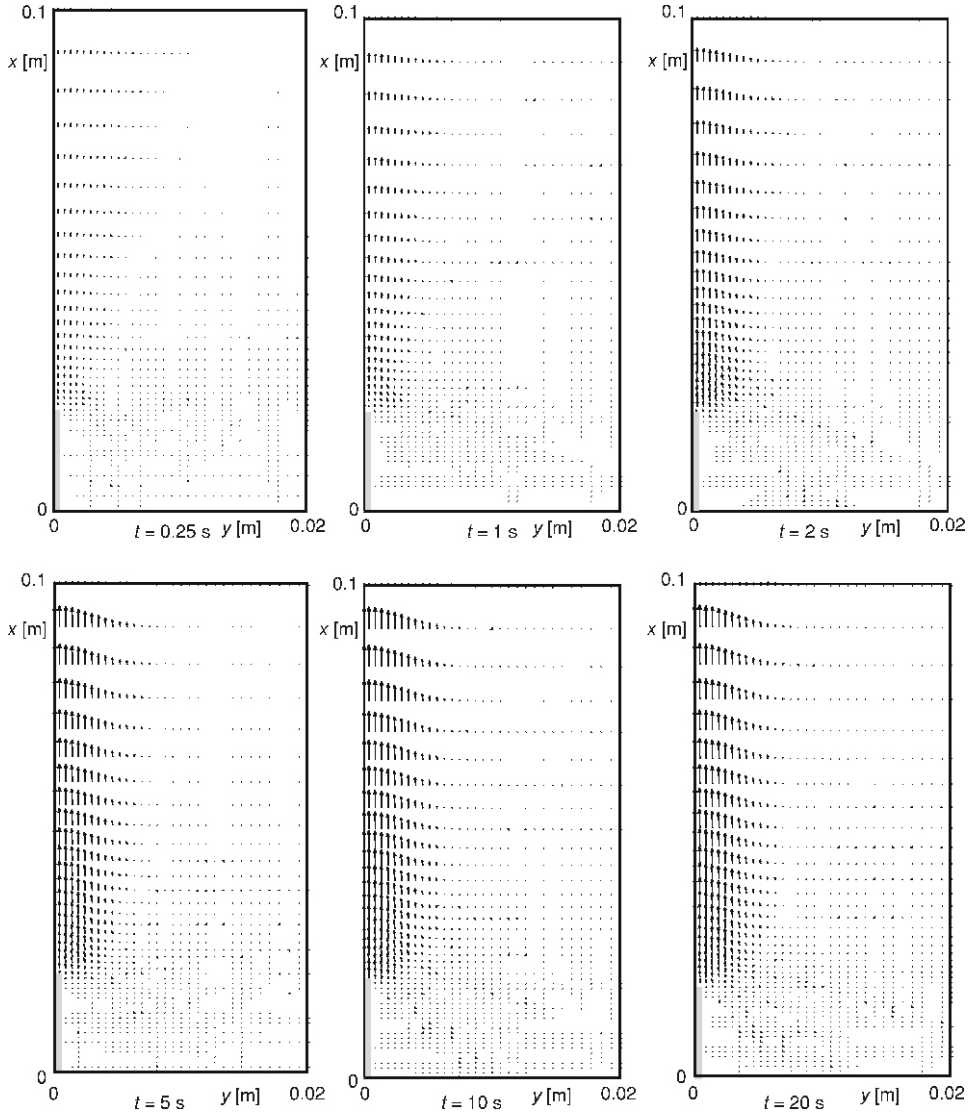

Figure 14. The variation of velocity vector in the computational domain *vs.* time (1 cm = 4 m/s)

vector takes place in the top boundary of computational domain beyond the early times. During 0 to 5 s, the velocity of flow field increases due to buoyancy force and beyond that time till to 20 s, there is not any obvious changes in the velocity of the flow field that represents the flow field reaches to steady-state situation.

The variation of isotherms in the computational domain *vs.* time is shown in fig. 15. This figure also shows the isotherms grow from 0 to 5 s and after 5 s reach to steady-state situation. In the early times (0-1 s) conduction to be dominates in the gas phase, thus the isotherms grow slowly and they have approximately a circular shape. The energy transfers through the gas phase between about 1 to 1.5 s faster than the early times because the advection mode of energy to be dominates in the flow field and hence the isotherms grow faster than the early times. The isotherms suddenly grow between 1.5 to 2 s

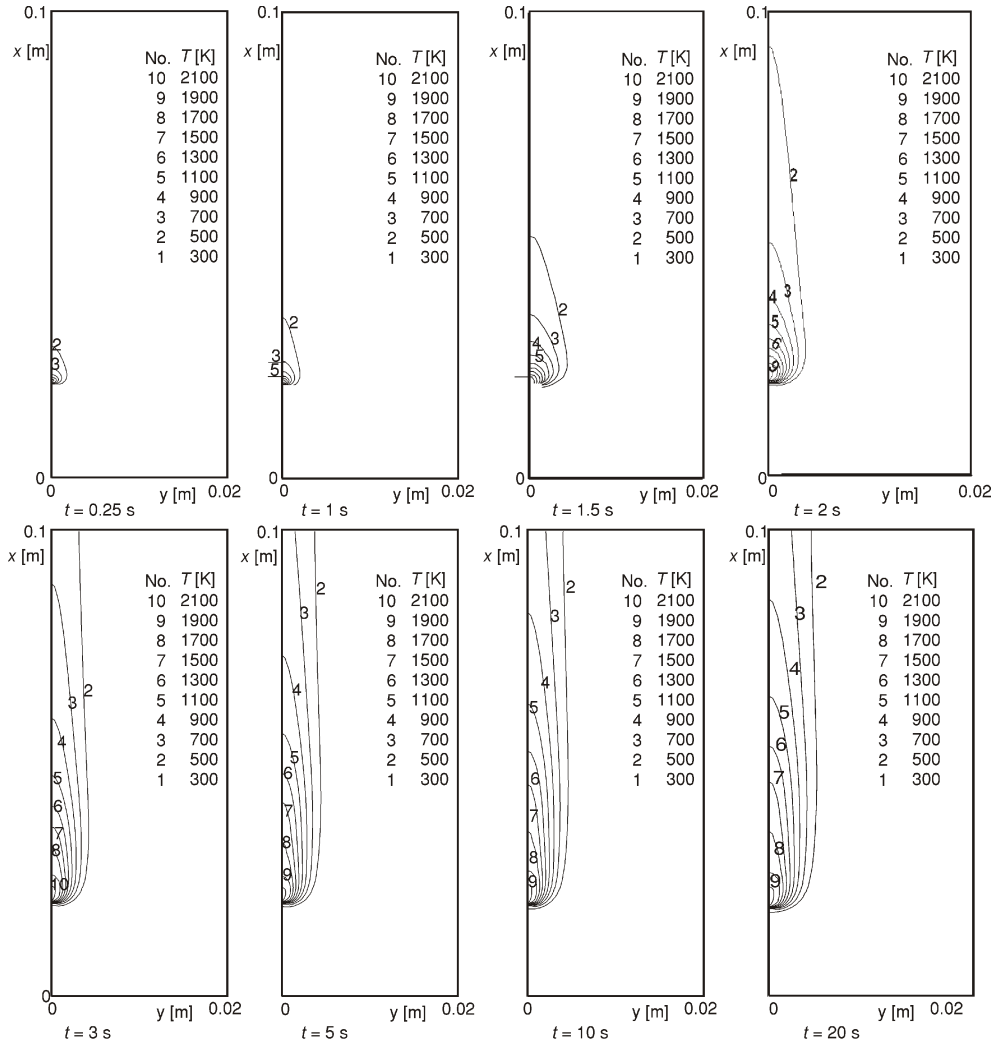

Figure 15. The variation of isotherms in computational domain *vs*. time

that is concerned to the threshold of combustion in the gas phase. This trend is continued till to reach steady-state situation.

Figure 16 shows the variation of Y_F in the symmetric plane *vs*. time. This figure shows the degradation in the solid fuel takes place beyond the first second and therefore the Y_F in the symmetric plane to be growing after 1 s and beyond 5 s actually that quantity does not change. That figure also shows the maximum value of Y_F is takes placed in the vicinity of the solid phase and its value decreases with increasing the height from the solid surface. This means the flame does not forms just on the solid surface, but it forms within a small distance from that surface. The variation of Y_F maximum location in fig. 16 is concerned to the reduction of solid fuel height due to burning.

The variation of Y_O in the symmetric plane *vs*. time are shown in fig. 17. This figure are also confirmed the results of fig. 16. The value of Y_O in the symmetric plane approximately is constant in the early times ($Y_O = Y_{O\infty}$). Beyond 1 s, its value decreases to reaches steady-state situation. As shown in fig. 17 the minimum value of Y_O at the symmetric plane (y 0) is occurred in a region near the solid surface that the height of it increases with respect to time till to reaches to the steady-state situation. This phenomenon concerned to the growth of flame size in the threshold of combustion, because that region is the flame region. This figure also shows the flame is apart from the solid surface.

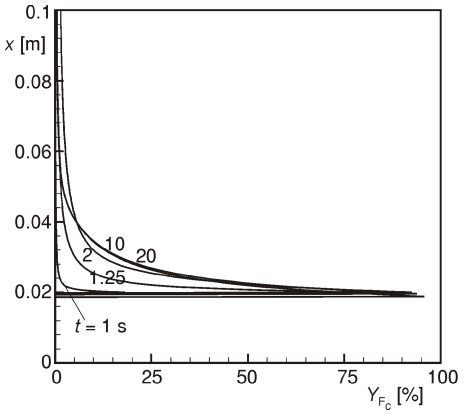

Figure 16. The variation of concentration of volatiles at the symmetric plane *vs*. time

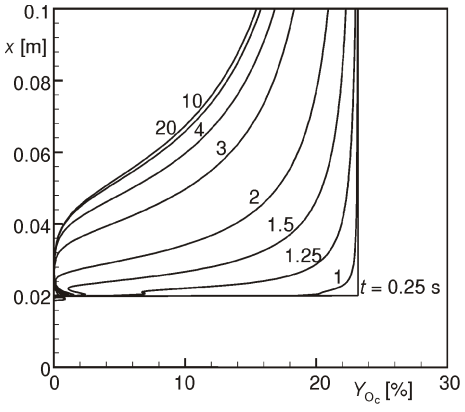

Figure 17. The variation of concentration of oxygen at the symmetric plane *vs.* time

The effect of surface regression on the results is shown in figs. 18-20. Figure 18 shows the variation of solid surface temperature and gas temperature in the vicinity of that surface with and without using of surface regression models *vs*. time. The regression surface of solid has more effect in the plateau region of those curves. The solid surface regression causes to increase the solid surface temperature and decrease the gas temperature in the vicinity of top solid surface. The solid density is assumed to be constant when the surface regression is not considered. Since the mass flux of volatiles is proportional to the solid density (eq. 17) then the surface regression causes to decrease that mass flux and

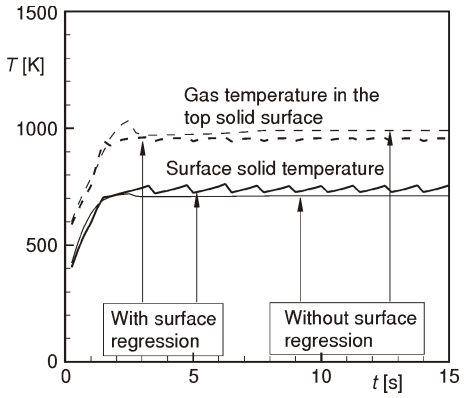

Figure 18. The effect of surface regression on the solid surface and gas temperature

the transfer of energy by advection mode through the solid phase. This phenomenon causes to increase the solid surface temperature that is shown in fig. 18. Also the reduction of mass flux of volatiles in this model cause to decrease the rate of chemical reaction and heat release due to combustion and therefore cause to decrease the gas temperature as shown in fig. 18. Then the temperature difference between the gas and solid phases with using the surface regression model is less than that difference without using the surface regression model (fig. 18). On the other hand, heat diffusion to the solid phase with using the surface regression model is less than that heat without using that model. But as shown before, the advection mode of energy without using the surface regression model is more than that mode of energy with using that model. Since diffusion mode of heat to the solid phase dominates to the advection mode of energy through that phase, it is expected the net energy transferred to the solid phase without using the surface regression model should be more than that energy with using that model. This fact is completely shown by fig. 19 that is represents the variation of net energy transferred to the solid phase *vs*. time with and without using the surface regression models.

As mentioned before, it is expected the mass flux of volatiles on the solid surface and therefore the volatiles velocity at that location without using the surface regression model should be more than that parameter with using that model. Figure 20 shows the variation of volatiles velocity with and without using the surface regression models *vs*.

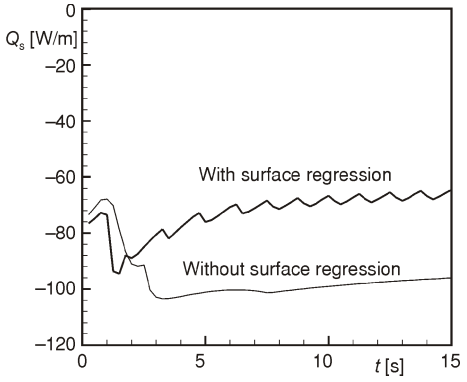

Figure 19. The effect of surface regression on the net energy transfer to the solid

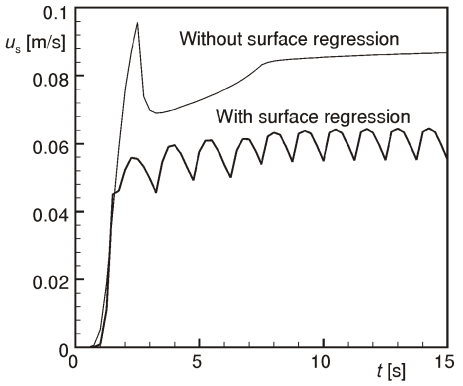

Figure 20. The effect of surface regression on the volatiles velocity on the solid surface

time. This figure confirms the mentioned physical results especially in the plateau region of the curves.

Concluding remarks

A numerical model is developed for the flame spread over a solid fuel in a quiescent ambient. The transient governing equations – mass, momentum, energy, and species were solved for both gas and solid (fuel) phases simultaneously. This model consist the effect of surface regression of the solid fuel. Based on this model, the following conclusions can be drawn:

– the surface regression of the solid fuel has effect on the solid surface temperature, mass flux of volatiles and velocity of volatiles on the solid surface, net energy transfer to the solid, *etc.*,
– the surface regression numerical model represents that phenomenon takes place step by step and it is assumed the solid height reduces discretely by a solid mesh size due to burning. This model causes to create some wiggles in the results in the plateau regions of curves, which those regions are concerned to the steady-state situation,
– the amplitude of wiggles on the results depend upon the solid mesh size, which its value is reduced monotonically with decreasing of solid mesh size so that if the solid mesh size approaches to zero, it can be predicted, the wiggles will be removed completely,
– all of the results are independent of solid mesh size for the solid mesh size less than 0.07 mm and all of them are independent of time step for time step less than 0.25 s, and
– the numerical model seems to provide valid predictions.

However, one important caution is required; thermal, thermo-physical, and chemical properties of solid fuel and gas were obtained from literature source, have many effect on the results.

Nomenclature

A – pre-exponential factor, [s^{-1}]
c – specific heat, [$Jkg^{-1}K^{-1}$]
c_p – specific heat at constant pressure for gas phase, [$Jkg^{-1}K^{-1}$]
D_{AB} – binary diffusion coefficient, [m^2s^{-1}]
E – activation energy, [Jkg^{-1}]
$\dot{G}$ – rate of energy generation due to chemical reaction, [Wm^{-3}]
H – height of computational domain, [m]
k – thermal conductivity, [$Wm^{-1}K^{-1}$]
L – height of solid fuel, [m]
M – molecular weight, [$g\,mol^{-1}$]
m'' – mass flux of volatiles on the solid fuel, [$kgm^{-2}s^{-1}$]
Pr – Prandtl number, [–]
p – pressure, [Nm^{-2}]

Q – total heat release due to combustion, [Wm^{-1}]
Q_{max} – maximum of total heat release due to combustion, [Wm^{-1}]
R – universal gas constant, [$J\,mol^{-1}K^{-1}$]
S – rate of pyrolysis reaction, [$kg\,m^{-2}s^{-1}$]
T – temperature, [°C], [K]
t – time, [s]
u – velocity component in the x direction, [ms^{-1}]
$\vec{V}$ – velocity vector, [ms^{-1}]
V_F – regression rate, [ms^{-1}]
v – velocity component in the y direction, [ms^{-1}]
X – body force in the x direction, [$kgm^{-2}s^{-2}$]
x – coordinate along vertical direction, [m]
Y – mass fraction, [–]
y – coordinate along horizontal direction, [m]
W – width of computational domain, [m]

Greek symbols

ΔH – heat of degradation, [$Jmol^{-1}$]
Δh – heat of combution, [$Jmol^{-1}$]
μ – dynamic viscosity, [$kgm^{-1}s^{-1}$]
ν – stoichiometric ratio, [–]
ρ – density, [kgm^{-3}]
σ – normal stress, [Nm^{-2}]
τ – shear stress, [Nm^{-2}]

Subscripts

c – center plane (symmetric plane)
F – fuel
g – gas
i – chemical species
O – oxygen
s – solid
v – volatiles
0 – initial condition
∞ – ambient

References

[1] Di Blasi, C., Modeling and Simulation of Combustion Processes of Charring and Non-Charring Solid Fuels, *Progress Energy Combustion Science, 19* (1993), 1, pp. 71-104
[2] Wichman, I. S., Theory of Opposed-Flow Flame Spread, *Progress Energy Combustion Science, 18* (1992), 6, pp. 553-593
[3] Fernandez-Pello, A. C., Williams, F. A., Laminar Flame Spread over PMMA Surfaces, *Proceedings*, 15th Symposium (Int.) on Combustion, 1974, The Combustion Institute, Pittsburgh, Pa., USA, 1975, pp. 217-231
[4] Mao, C. P., Kodama, H., Fernandez-Pello, A. C., Convective Structure of a Diffusion Flame over a Flat Combustible Surface, *Combustion and Flame, 57* (1984), 2, pp. 209-236

[5] Bhattacharjee, S., Altenkirch, R. A., Srikantaiah, N., Vedha-Nayagam, M., A Theoretical Description of Flame Spreading over Solid Combustible in a Quiescent Environment at Zero Gravity, *Combustion Science and Technology, 69* (1990), 1, pp. 1-15
[6] Bhattacharjee, S., Altenkirch, R. A., Radiation-Controlled, Opposed-Flow Flame Spread in a Microgravity Environment, *Proceedings*, 23th Symposium (Int.) on Combustion, 1990, The Combustion Institute, Pittsburgh, Pa., USA, 1991, pp. 1627-1633
[7] Di Blasi, C., Crescitelli, S., Russo, G., Cinque, G., Numerical Model of Ignition Processes of Polymeric Materials Including Gas-Phase Absorption of Radiation, *Combustion and Flame, 83* (1991), 3, pp. 333-344
[8] Bhattacharjee, S., Altenkirch, R. A., A Comparison of Theoretical and Experimental Results in Flame Spread over Thin Condensed Fuels in a Quiescent, Microgravity Environment, *Proceedings*, 24th Symposium (Int.) on Combustion, 1992, The Combustion Institute, Pittsburgh, Pa., USA, 1993, pp. 1669-1676
[9] Ramanchandra, P. A., Altenkirch, R. A., Bhattacharjee, S., Tang, L., Sacksteder, K., Wolverton, M. K., The Behavior of Flame Spreading over Thin Solids in Microgravity, *Combustion and Flame, 100* (1995), 1, pp. 71-84
[10] Bhattacharjee, S., Altenkirch, R. A., Sacksteder, K., The Effect of Ambient Pressure on Flame Spread over Thin Cellulosic Fuel in a Quiescent, Microgravity Environment, *J. of Heat Transfer, 118* (1996), 1, pp. 181-190
[11] Jiang, C. B., Tien, J. S., Shih, H., Model Calculation of Steady upward Flame Spread over a Thin Solid in Reduced Gravity, *Proceedings*, 26th Symposium (Int.) on Combustion, 1996, The Combustion Institute, Pittsburgh, Pa., USA, 1997, pp. 1353-1360
[12] Altenkirch, R. A., Tang, L., Sacksteder, K., Bhattacharjee, S., Delichatsios, M. A., Inherently Unsteady Flame Spread to Extinction over Thick Fuels in Microgravity, *Proceedings*, 27th Symposium (Int.) on Combustion, 1998, The Combustion Institute, Pittsburgh, Pa., USA, 1999, pp. 2515-2524
[13] Esfahani, J. A., Sousa, A. C. M., Ignition of Epoxy by a High Radiation Source: A Numerical Study, *Int. J. Thermal Science, 38* (1999), 4, pp. 315-323
[14] Sousa, A. C. M., Esfahani, J. A., Numerical Modeling of PMMA Ignition Induced by Monochromatic Radiation, *Proceedings*, 17th UIT National Heat Transfer Conference, Ferrara, Italy, 1999, pp. 409-420
[15] Esfahani, J. A., Oxygen-Sensitive Thermal Degradation of PMMA: A Numerical Study, *Combustion Science and Technology, 174* (2002), 10, pp. 183-198
[16] Esfahani, J. A., Ayani, M. B., Bakht Shirin, M., A Transient Two-Dimentional Model of Thermal and Oxidative Degradation of PMMA, *Iranian J. of Science and Technology, Transaction B, Engineering, 29* (2005), B2, pp. 207-218
[17] Esfahani, J. A., Kashani, A., A Numerical Model for Degradation and Combustion of Polymethy lmethacrylate (PMMA), *Heat and Mass Transfer, 42* (2006), 6, pp. 569-576
[18] Glassman, I., Combustion, 3rd ed., Academic Press, Oxford, UK
[19] Anderson, J. D., Jr., Fundamentals of Aerodynamics, 2nd ed., Mac Graw-Hill, New York, USA, 1991
[20] Patankar, S.V., Numerical Heat Transfer and Fluid Flow, McGraw-Hill, New York, USA, 1980
[21] Van Doormaal, J. P., Raithby, G. D., Enhancements of the SIMPLE Method for Predicting Incompressible Fluid Flows, *Numerical Heat Transfer, Part B, 7* (1984), 2, pp. 147-163
[22] Thakur, S., Shyy, W., Some Implementation Issues of Convection Schemes for Finite-Volume Formulations, *Numerical Heat Transfer, Part B, 24* (1993), 1, pp. 31-55
[23] Ito, A., Kashiwagi, T., Temperature Measurements in PMMA during Downward in Flame Spread in Air Using Holographic Interferometry, *Proceedings*, 21st Symposium (Int.) on Combustion, 1985, The Combustion Institute, Pittsburgh, Pa., USA, 1986, pp. 65-74

Authors' addresses:

M. B. Ayani, J. A. Esfahani
Department of Mechanical Engineering
Ferdowsi University of Mashhad
P. O. Box 91775-1111, Mashhad, Iran

A. C. M. Sousa
Department of Mechanical Engineering
University of New Brunswick
P. O. Box 4400, Fredericton, NB, Canada, E3B 5A3

Corresponding author J. A. Esfahani
E-mail: abolfazl@um.ac.ir or jaesfahani@gmail.com

Paper submitted: February 20, 2006
Paper revised: March 30, 2006
Paper accepted:May 1, 2006